Effects of substrate rotation in oblique-incidence metal(100) epitaxial growth

Yunsic Shim,[1,*] Mary E. Mills,[1,2] Valery Borovikov,[1,†] and Jacques G. Amar[1,‡]
[1]*Department of Physics and Astronomy, University of Toledo, Toledo, Ohio 43606, USA*
[2]*College of Wooster, Wooster, Ohio 44691, USA*
(Received 2 March 2009; published 8 May 2009)

The effects of substrate rotation on the surface morphology in oblique-incidence metal(100) epitaxial growth are studied via kinetic Monte Carlo simulations of a simplified model, and compared with previous results obtained without rotation. In general, we find that substrate rotation leads to two main effects. At high deposition angles with respect to the substrate normal, rotation leads to a significant change in the surface morphology. In particular, it leads to isotropic mounds and pyramids with (111) facets rather than the anisotropic ripples and rods observed in the absence of rotation. Due to the existence of rapid transport on these facets, the lateral feature size increases approximately linearly with film thickness. Due to the fact that substrate rotation tends to reduce the effects of shadowing, the surface roughness is also decreased compared to the roughness in the absence of rotation. While this leads to a moderate reduction in the roughness for the case of ballistic deposition, the effect is significantly larger in the case of deposition with attraction. In the case of ballistic deposition, we also find that the surface roughness increases with rotation rate Ω for $\Omega < 1$ rev/monolayer (ML) before saturating at larger rotation rates ($\Omega > 1$ rev/ML). In contrast, for the case of attraction the surface roughness exhibits a negligible dependence on rotation rate for finite rotation rate.

DOI: 10.1103/PhysRevE.79.051604 PACS number(s): 81.15.Aa, 68.55.−a, 81.10.Aj

I. INTRODUCTION

During the last two decades there has been a lot of progress made in understanding the detailed mechanisms controlling the surface morphology in epitaxial growth [1,2]. Besides the existence of a variety of activated processes which can affect the growth morphology (such as the Ehrlich-Schwoebel barrier to interlayer diffusion [3] and edge and corner diffusion [4–6]), recently it has been shown that the deposition process can also play an important role, especially at low temperatures and/or large deposition angles. For example, recent glancing angle deposition experiments on Cu/Cu(100) growth by van Dijken *et al.* [7,8] demonstrate a dramatic dependence of the surface morphology on deposition angle, including a transition from symmetric to asymmetric mounds, and finally to ripples oriented perpendicular to the beam with increasing deposition angle. In addition, a variety of theoretical studies [9–18] have shown that interactions between the deposited atom and the surface can have a significant effect on the surface morphology.

Recently, using a simplified ballistic deposition model [17] which includes the effects of downward funneling (DF) [19] and rapid diffusion on (111) facets, two of us have shown that many of the qualitative and semiquantitative features observed in high-angle oblique-incidence growth by van Dijken *et al.* [7,8], can be explained primarily by shadowing effects. In addition, our simulations indicate the existence of a second transition for large deposition angles and film thicknesses from ripples oriented perpendicular to the beam to "rods" oriented parallel to the beam [20]. More recently, we have also studied the modifying effects of short-range (SR) and long-range (LR) attraction on the surface morphology [18]. While shadowing still plays an important role, at large deposition angles we find that attraction can have two important effects. The first effect, which is a result of steering due to LR attraction, leads to decreased shadowing and anisotropy in the submonolayer regime and can also lead to decreased surface roughness for high deposition angles at intermediate film thicknesses. The second effect, due to flux focusing, leads to an increase in the surface roughness and also reduces the critical thickness for ripple and rod formation. This effect also tends to limit the anisotropy in the rod phase for high deposition angles and film thicknesses. Seo *et al.* [15] have also pointed out that steering due to attraction can affect the surface morphology of Cu/Cu(100) epitaxial films.

We note that in the oblique-incidence epitaxial growth experiments considered so far, the substrate is typically held fixed. As a result, both the deposition angle θ with respect to the substrate normal and the azimuthal angle ϕ are constant. However, in a number of cases of nonepitaxial growth, such as glancing angle deposition (GLAD) [21], substrate rotation has been used to control and or alter the surface morphology. Therefore, it is interesting to examine how substrate rotation may alter the general picture obtained for the case of oblique-incidence epitaxial metal (100) growth. Accordingly, here we present the results of simulations of a simplified model of oblique-incidence epitaxial metal (100) growth at high deposition angles, which includes the effects of substrate rotation. In particular, we have studied the effects of substrate rotation (see Fig. 1) on the surface morphology and surface roughness for large deposition angles $\theta \geq 70°$, both in the presence of LR and SR attraction and in the absence of attraction (ballistic deposition). We note that while the model studied here is in some sense generic, many of the parameters are close to or similar to those expected for Cu/Cu(100) and Fe/Fe(100) growth at or somewhat below room temperature. Therefore, we expect that our results will be relevant to

*yshim@physics.utoledo.edu
†vborovikov@physics.utoledo.edu
‡jamar@physics.utoledo.edu

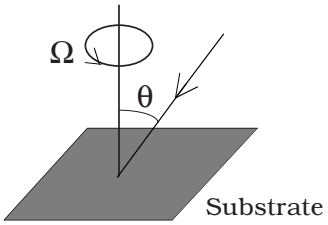

FIG. 1. Schematic diagram showing deposition angle θ and substrate rotation with rate $\Omega = d\phi/dt$.

experiments on oblique-incidence metal(100) epitaxial growth in the presence of rotation.

As discussed in more detail below, our results indicate that substrate rotation can dramatically affect the surface morphology. In addition, we find that substrate rotation tends to reduce the surface roughness moderately in the case of ballistic deposition and even more significantly in the case of deposition with attraction. Somewhat surprisingly, we also find that while the surface roughness is reduced in the presence of rotation, it depends relatively weakly on rotation rate Ω for $\Omega > 1$ rev/monolayer (ML). More importantly, we find that the ripples or rods observed [17,18] in oblique-incidence simulations without substrate rotation do not appear in the presence of substrate rotation. Instead, well-developed pyramids are observed with (111) facets whose lateral size increases rapidly as the deposition angle increases. In the case of attraction, these pyramids are relatively well ordered while their size distribution corresponds approximately to a bimodal distribution.

The organization of this paper is as follows. In Sec. II, we describe the model used in our simulations along with a summary of the simulation parameters. We then present our results in Sec. III. Finally, in Sec. IV, we summarize our results.

II. MODEL AND SIMULATIONS

In order to compare with previous results for deposition at oblique incidence without rotation, we have used the same kinetic Monte Carlo model as was previously used in Ref. [18]. We note that this model is similar to previous models [22,23] used to study metal (100) growth at normal incidence in which the fcc crystal geometry has been taken into account. In particular, atoms are deposited with a (per site) deposition rate F, while adatoms (monomers) on a flat terrace are assumed to diffuse with hopping rate D. The rate for an adatom at a descending step edge to diffuse over the step is given by $D_{\mathrm{ES}} = De^{-E_{\mathrm{ES}}/k_B T}$, where E_{ES} is the Ehrlich-Schwoebel barrier and k_B is the Boltzmann's constant. Compact islands are also assumed and accordingly a moderate amount of edge and corner diffusion ($D_e = D_c = 0.01D$) was included, while the attachment of atoms to existing islands was assumed to be irreversible. We note that in the case of Cu/Cu(100) the barrier for edge diffusion is significantly lower than for monomer diffusion, while the rate of corner diffusion is almost as large as that for monomer diffusion. The resulting fast edge diffusion leads to large regular mounds whose gaps are further enhanced by flux focusing. However, we do not expect these effects to alter the qualitative behavior discussed here.

Besides the deposition angle and rotation rate, two of the key parameters in this model are the ratio D/F of the monomer diffusion rate to the deposition rate, and the magnitude of the ES barrier. In our simulations, a deposition rate corresponding to $D/F = 10^5$ was used and a moderate ES barrier corresponding to $E_{\mathrm{ES}} = 0.07$ eV at room temperature was assumed. We note that this value of D/F is in good agreement with that expected for the experiments of van Dijken *et al.* [7,8] on oblique-incidence Cu/Cu(100) growth with deposition rate $F \simeq 0.0042$ ML/s and $T \simeq 240$ K and is also in good agreement with experiments on room-temperature mound formation in Fe/Fe(100) growth at normal incidence [24,25].

To distinguish between the effects of shadowing and attraction, we have carried out simulations both with SR and LR attraction as well as without attraction (ballistic deposition). In both cases, the depositing atom was launched from a random position above the substrate at a height equal to the height of the highest point of the film plus the LR cutoff distance r_{cut} with the appropriate deposition angle θ with respect to the substrate normal and azimuthal angle ϕ. A one-atom molecular-dynamics (MD) simulation of the trajectory of the depositing atom was then carried out (with the substrate atoms all held fixed at their lattice positions) until the distance of the depositing atom to the closest substrate atom was equal to the nearest-neighbor distance $a_1 = a/\sqrt{2}$ (where a is the crystal lattice constant). If the empty lattice site above this substrate atom corresponds to a fourfold hollow site, the depositing atom is moved to this site, otherwise it is assumed to "cascade" randomly via downward funneling (DF) [19] until it reaches a fourfold hollow site. Thus, in our model atoms deposited on (111) microfacets are assumed to diffuse essentially instantaneously via DF to the terrace below. When considering the extremely low barriers for diffusion on metal (111) surfaces (approximately 0.05 eV for Cu(111) [26]), this is a very reasonable approximation except at very low temperature.

As in Ref. [18], for the case of attraction the initial kinetic energy of the deposited atom was chosen to correspond approximately to that for Cu/Cu(100) deposition, i.e., $\bar{K}_i = 0.2$ eV. As in several previous simulations of steering effects in Cu/Cu(100) growth [11,12,14], in this case a Lennard-Jones (LJ) copper potential [27], given by

$$V_{\mathrm{LJ}}(r) = 4\epsilon\left[\left(\frac{\sigma}{r}\right)^{12} - \left(\frac{\sigma}{r}\right)^{6}\right] \tag{1}$$

(where $\epsilon = 0.4093$ eV and $\sigma = 2.3377$ Å) was used to represent the SR interaction. Similarly, to take into account the LR van der Waals attraction [28] an additional pair interaction of the form $V_{\mathrm{LR}} = -\gamma/r^6$ (using the value $\gamma = 47.2$ eV-Å^6 previously obtained for Cu in Ref. [28]) was included for atoms which are farther than the cutoff distance for the short-range interaction. To avoid a discontinuity between the short-range $V_{\mathrm{LJ}}(r)$ and long-range $V_{\mathrm{LR}}(r)$ potentials we have used the following expression for the pair-potential in our simulations:

$$V_T(r) = [1 - f(r)]V_{\mathrm{LJ}}(r) + f(r)V_{\mathrm{LR}}(r), \quad (2)$$

where $f(r)=1/[1+e^{-(r-2\sigma)/R}]$ is the sigmoid function centered on $r=2\sigma$ with width $R=0.125\sigma$. However, we note that the results were relatively insensitive to the value of R. To save computation time in our calculations of the pair interaction, a long-range cutoff $r_{\mathrm{cut}}=7\sigma$ was used, since the results were found not to depend on the cutoff for larger values.

In order to examine the dependence of the surface morphology on deposition conditions we have calculated a variety of different quantities as a function of the average film thickness t in MLs, deposition angle θ and rotation rate Ω. These include the r.m.s. surface height or "width" w, and the circularly averaged correlation length ξ_c determined from the first zero-crossing of the circularly averaged correlation function $G(r)=\langle\tilde{h}(0)\tilde{h}(r)\rangle$, where $h(\mathbf{r})$ is the surface height at position $\mathbf{r}$ and $\tilde{h}(\mathbf{r})=h(\mathbf{r})-\bar{h}$ is the deviation from the average height. For the case of ballistic deposition our results were averaged over 10–100 runs, while for the more time-consuming case of deposition with attraction our results were averaged over 5 runs.

In order to study the dependence on rotation rate, results were obtained for rotation rates Ω ranging from values much less than 1 rev/ML and as high as 5 rev/ML. In addition, simulations with a random azimuthal deposition angle (corresponding to the limit of a very large rotation rate) were also carried out. We note that in previous simulations of oblique-incidence growth with attraction but without substrate rotation [18] it was found that there was a negligible dependence of the surface roughness on the azimuthal angle. Accordingly, for the comparison case of no rotation, simulations with a fixed azimuthal angle $\phi=45°$ corresponding to the [110] direction were carried out. This is the same azimuthal direction as was used in the experiments of Refs. [7,8]. To minimize finite-size effects, relatively large system sizes ($L=512$ in units of the lattice spacing) were used.

III. RESULTS

A. Dependence of roughness on rotation rate

We first discuss the effects of substrate rotation on the surface roughness. As can be seen from Fig. 2, in general substrate rotation leads to a reduced surface roughness when compared to the case of no rotation (solid curves). This is due to the fact that rotation tends to reduce the amount of shadowing, thus, reducing the roughness. However, the decrease in the surface roughness due to rotation is typically larger in the case of attraction than for ballistic deposition. This is not surprising since in the absence of rotation, the effects of shadowing and attraction reinforce each other, i.e., shadowing leads to increased flux focusing, thus increasing the surface roughness, which leads to further shadowing. However, in the presence of rotation the decreased amount of shadowing leads to a decrease in flux focusing, thus further reducing the surface roughness. Consistent with this observation, a comparison of Figs. 2(a) and 2(b) also indicates that for a given deposition angle θ the surface roughness is higher in the case of attraction than in the case of ballistic deposition [18].

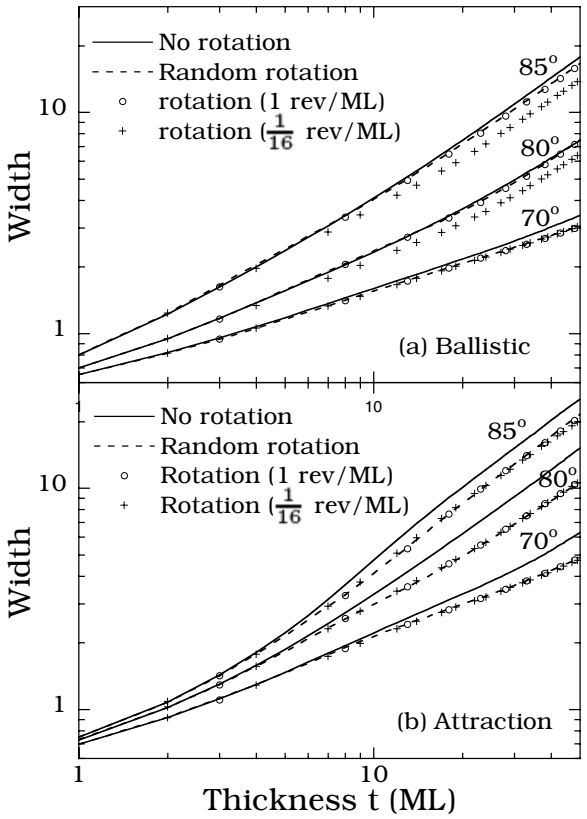

FIG. 2. Surface roughness as function of film thickness for $\theta=70°-85°$ (a) without (ballistic deposition) and (b) with attraction for cases of no rotation, random rotation and rotation with rates $\Omega=\frac{1}{16}$ and 1 rev/ML.

Figure 3 shows the relative deviation in the width $w(t,\theta,\Omega)/w(t,\theta,0)-1$ compared to the width in the absence of rotation at $t=25$ ML and 50 ML as a function of the rotation rate Ω for several different deposition angles $\theta=70°$, 80°, and 85°. Results are shown for both ballistic deposition and deposition with attraction. As can be seen, in the case of ballistic deposition the roughness tends to increase with rotation rate for small Ω and then saturate for $\Omega \geq 1$ rev/ML at a value which is lower than in the absence of rotation. As a result, the smallest roughness occurs for the smallest nonzero rotation rate ($\Omega=1/16$ rev/ML) while the largest roughness occurs in the absence of rotation ($\Omega=0$). However, while the surface roughness is lower in the presence of rotation than in the absence of rotation in the case of attraction, there is a negligible dependence on rotation rate for $\Omega \neq 0$. One possible explanation for this difference is as follows. For small rotation rates $\Omega<1$ rev/ML, rotation forces the mounds to grow in a spiral fashion as the substrate is rotated. In the case of ballistic deposition, this "spiral growth" tends to fill-in the gaps between mounds, thus, reducing the surface roughness. As the rotation rate increases, the amount of spiral growth is reduced, thus, leading to an increase in the surface roughness. In contrast, in the case of attraction, the feature sizes are typically much larger and deeper due to flux focusing. As a result, the existence of "spiral" mound growth due to rotation has a negligible effect on the surface roughness.

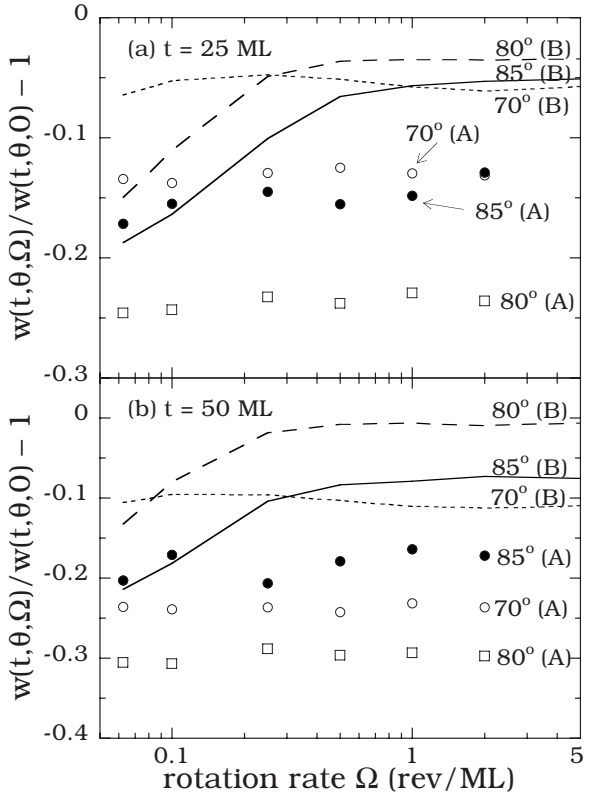

FIG. 3. Relative width deviation $\delta w/w(t,\theta,0)$ as function of rotation rate Ω with and without attraction, where A and B in parentheses stand for attraction and ballistic deposition, respectively. (a) $t=25$ ML and (b) $t=50$ ML.

B. Dependence of surface morphology on rotation rate

We now consider the effects of substrate rotation on the surface morphology. Figure 4 shows a comparison of the surface morphology at a film thickness of 50 ML for the case of ballistic deposition for different rotation rates Ω and deposition angles θ. As previously observed in Ref. [17], in the absence of rotation ($\Omega=0$) a series of morphological transitions occurs with increasing deposition angle from asymmetric mounds at $\theta=70°$ (not shown) to asymmetric ripples running perpendicular to the beam with (111) facets on the illuminated side at $\theta=80°$, and finally to rotated rods with (111) front and side facets at $\theta=88°$. In the presence of substrate rotation, however, these orientational transitions are suppressed. Instead, as can be seen in Fig. 4, for the case of large rotation rate ($\Omega=1$ rev/ML), a gradual transition occurs with increasing deposition angle from fuzzy or poorly developed mounds at $\theta=80°$ to more well-developed mounds at $\theta=85°$ and finally to well-defined pyramidal mounds with sharp tips and (111) side facets at $\theta=88°$. Thus, the ripples or rods formed at high deposition angles in the absence of rotation are replaced by well-defined mounds and pyramids in the presence of rotation. We note that in the case of slow rotation ($\Omega<1$ rev/ML) the observed mounds are less regular and well developed than for higher rotation rates. In addition, in this case some of the mound tops are relatively flat or contain small dimples, in contrast to the case of fast rotation for which the tops tend to be sharper and more regular.

Similar results are shown in Fig. 5 for the case of attraction. We note that in this case, due to flux focusing, the pyramids are relatively well-developed with sharp tops and well-defined (111) facets, while the corresponding feature sizes are larger than in the case of ballistic deposition. We also note that for the largest deposition angles ($\theta=85°$ and 88°) there exists a bimodal distribution of mound sizes with a number of smaller mounds as well as large mounds with well-defined (111) facets.

In order to quantify the lateral mound size and/or feature size, we have calculated the circularly averaged correlation length ξ_c as a function of film thickness for different rotation rates and deposition angles $\theta=70°-88°$ with and without attraction. As can be seen in Fig. 6, for a given deposition angle the correlation length ξ_c for the case of attraction is larger than that for the case of ballistic deposition due to flux focusing. In addition, we find that ξ_c increases approximately linearly after an initial transient period which is related to the formation of (111) facets on the sides of pyramids. Once such (111) facets are formed, atoms landing on these facets are efficiently transported to a lower terrace via DF, thus, leading to linear growth of the correlation length with coverage. We note that such linear behavior was also observed in the case of no substrate rotation with a deposition angle of $\theta=88°$ due to the formation of well-defined (111) facets on the front and sides of rods [17].

IV. CONCLUSION

We have presented the results of kinetic Monte Carlo simulations of a model of oblique-incidence metal(100) growth in the presence of substrate rotation in order to understand the effects of rotation on the surface morphology. We have also compared our results with those obtained in the absence of rotation. In general, two main effects are observed. At high deposition angles, substrate rotation results in a drastic change in the surface morphology. In particular, it leads to isotropic mounds and pyramids rather than the strongly anisotropic structures, such as ripples or rods, observed in the absence of rotation. Rotation also leads to a reduced surface roughness, although the surface roughness tends to increase with rotation rate.

We have also compared the effects of substrate rotation in the absence of attraction with the corresponding effects in the presence of attraction. For the case of ballistic deposition and large deposition angles ($\theta\geq 80°$), the decrease in the surface roughness (compared to the absence of rotation) is largest for a slow rotation rate ($\Omega=\frac{1}{16}$ rev/ML) and decreases with increasing rotation rate and then saturates for $\Omega\simeq\frac{1}{2}$ rev/ML. On the other hand, in the case of attraction there is a negligible dependence of the surface roughness on rotation rate for finite rotation rate. As already noted, this may be explained by the fact that flux focusing leads to feature sizes, which are much larger than in the case of ballistic deposition,

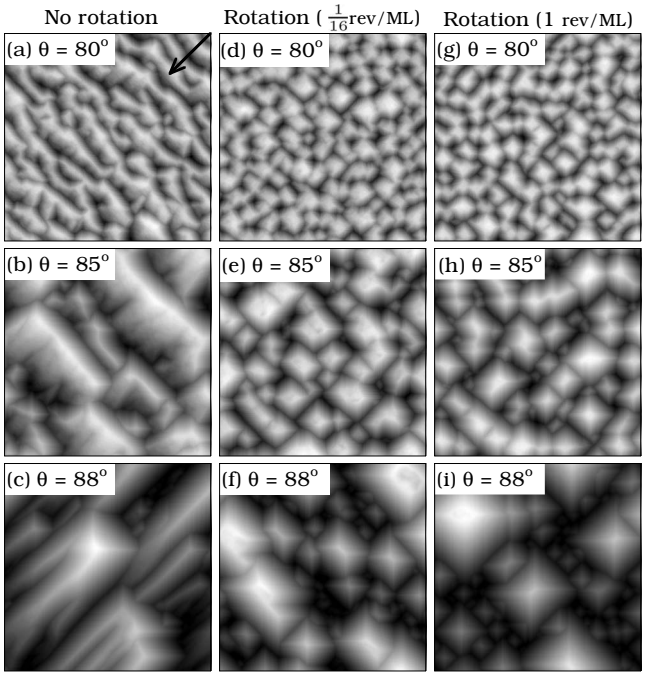

FIG. 4. Comparison of surface morphology for the case of ballistic deposition with and without substrate rotation for $\theta = 80° - 88°$ with $L=512$ at $t=50$ ML. Here, (a)–(c) correspond to no rotation while (d)–(f) and (g)–(i) correspond to rotation with $\Omega = 1/16$ rev/ML and 1 rev/ML, respectively. The arrow in (a) denotes deposition direction ($\phi=45°$) for the case of no rotation.

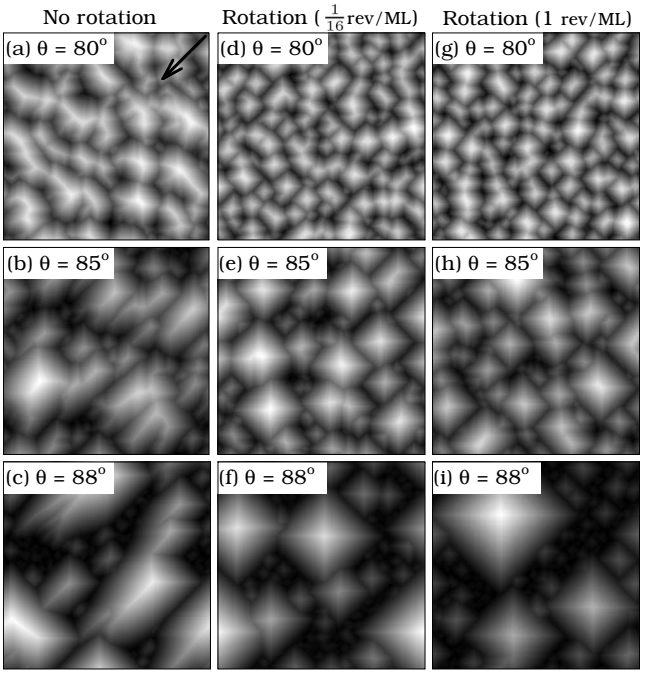

FIG. 5. Comparison of surface morphology for the case of attraction with and without substrate rotation for $\theta=80° - 88°$ with $L=512$ at $t=50$ ML. Here, (a)–(c) correspond to no rotation while (d)–(f) and (g)–(i) correspond to rotation with $\Omega=1/16$ rev/ML and 1 rev/ML, respectively. The arrow in (a) denotes deposition direction ($\phi=45°$) for the case of no rotation.

thus, reducing the effects of spiral mound growth on the surface roughness.

Similar differences between the morphology in the case of ballistic deposition and that in the case of attraction can also be noted in the presence of rotation. In particular, while rotation tends to promote the formation of (111) facets on the sides of mounds and pyramids in the case of attraction the resulting pyramids are larger and more well ordered than in the case of ballistic deposition. We also note that in the case of attraction with rotation, there appear to be a large number of relatively large pyramids as well as a relatively large number of much smaller pyramids, thus, leading to an approximately bimodal size distribution.

We have also carried out a detailed analysis of the circularly averaged correlation length which reveals that after an initial transient period related to the formation of (111) facets, the correlation length increases approximately linearly with film thickness. This linear behavior is associated with the rapid transport expected on a well-defined (111) facet. Thus, any process, such as attraction, which promotes the formation of (111) facets, leads to a significant increase in the correlation length and surface roughness.

In summary, we have shown that substrate rotation can dramatically alter the surface morphology in oblique-incidence metal(100) growth. In particular, the asymmetric ripples or rods observed at high deposition angles in the absence of substrate rotation are replaced by well-defined pyramids with (111) facets in the presence of rotation. Due to the existence of rapid transport on these facets, the lateral feature size increases approximately linearly with film thick-

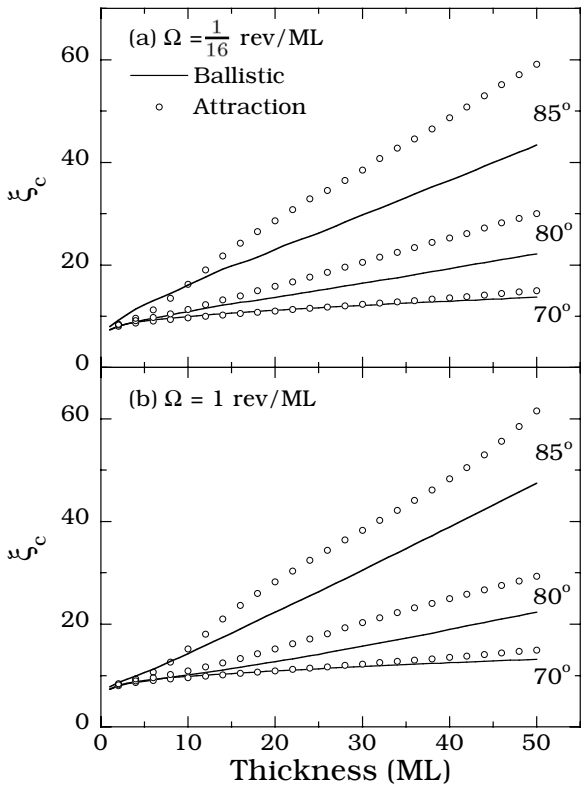

FIG. 6. Circularly averaged correlation length as a function of film thickness with (a) $\Omega=\frac{1}{16}$ rev/ML and (b) 1 rev/ML for deposition angles $\theta=70° - 85°$ with and without attraction. All results are for $D/F=10^5$ and $E_{ES}=0.07$ eV.

ness. We have also found that due to the fact that substrate rotation tends to reduce the effects of shadowing, the surface roughness is decreased compared to the roughness in the absence of rotation. While this leads to a moderate reduction in the surface roughness for the case of ballistic deposition, the effect is significantly larger in the case of deposition with attraction.

ACKNOWLEDGMENTS

M.E.M. gratefully acknowledges National Science foundation (NSF) funding for Research Experience for Undergraduates program. This work was also supported by NSF under Grant No. DMR-0606307 as well as by a grant of computer time from the Ohio Supercomputer Center.

[1] *Morphological Organization in Epitaxial Growth and Removal*, edited by Z. Zhang and M. G. Lagally (World Scientific, Singapore, 1998).
[2] J. W. Evans, P. A. Thiel, and M. C. Bartelt, Surf. Sci. Rep. **61**, 1 (2006).
[3] G. Ehrlich and F. G. Hudda, J. Chem. Phys. **44**, 1039 (1966); R. L. Schwoebel, J. Appl. Phys. **40**, 614 (1969).
[4] J. G. Amar, Phys. Rev. B **60**, R11317 (1999).
[5] M. V. Ramana Murty and B. H. Cooper, Phys. Rev. Lett. **83**, 352 (1999); M. V. Ramana Murty and B. H. Cooper, Surf. Sci. **539**, 91 (2003).
[6] O. Pierre-Louis, M. R. D'Orsogna, and T. L. Einstein, Phys. Rev. Lett. **82**, 3661 (1999).
[7] S. van Dijken, L. C. Jorritsma, and B. Poelsema, Phys. Rev. Lett. **82**, 4038 (1999).
[8] S. van Dijken, L. C. Jorritsma, and B. Poelsema, Phys. Rev. B **61**, 14047 (2000).
[9] M. Raible, S. J. Linz, and P. Hanggi, Phys. Rev. E **62**, 1691 (2000).
[10] F. Montalenti and A. F. Voter, Phys. Rev. B **64**, 081401(R) (2001).
[11] J. Yu and J. G. Amar, Phys. Rev. Lett. **89**, 286103 (2002).
[12] J. Seo, S.-M. Kwon, H.-Y. Kim, and J.-S. Kim, Phys. Rev. B **67**, 121402(R) (2003).
[13] M. Ceriotti, R. Ferrando, and F. Montalenti, Nanotechnology **17**, 3556 (2006).
[14] J. Seo, H.-Y. Kim, and J.-S. Kim, Phys. Rev. B **71**, 075414 (2005).
[15] J. Seo, H.-Y. Kim, and J.-S. Kim, J. Phys.: Condens. Matter **19**, 486001 (2007).
[16] V. Borovikov, Y. Shim, and J. G. Amar, Phys. Rev. B **76**, 241401(R) (2007).
[17] Y. Shim and J. G. Amar, Phys. Rev. Lett. **98**, 046103 (2007).
[18] Y. Shim, V. Borovikov, and J. G. Amar, Phys. Rev. B **77**, 235423 (2008).
[19] J. W. Evans, D. E. Sanders, P. A. Thiel, and A. E. DePristo, Phys. Rev. B **41**, 5410 (1990).
[20] We note that this second transition has since been experimentally observed [H. Woormeester (private communication)].
[21] A. Amassian, K. Kaminska, M. Suzuki, L. Martinu, and K. Robbie, Appl. Phys. Lett. **91**, 173114 (2007).
[22] J. G. Amar and F. Family, Phys. Rev. B **54**, 14742 (1996).
[23] Y. Shim and J. G. Amar, Phys. Rev. B **73**, 035423 (2006).
[24] Y. L. He, H. N. Yang, T. M. Lu, and G. C. Wang, Phys. Rev. Lett. **69**, 3770 (1992).
[25] J. A. Stroscio, D. T. Pierce, M. D. Stiles, A. Zangwill, and L. M. Sander, Phys. Rev. Lett. **75**, 4246 (1995).
[26] A. Bogicevic, S. Ovesson, P. Hyldgaard, B. I. Lundqvist, H. Brune, and D. R. Jennison, Phys. Rev. Lett. **85**, 1910 (2000).
[27] D. E. Sanders and A. E. DePristo, Surf. Sci. **254**, 341 (1991).
[28] J. G. Amar, Phys. Rev. B **67**, 165425 (2003).